Finite-volume effects on the chiral phase transition of thermal QED_3

Hong-tao Feng,[1,*] Yong-hui Xia,[2] and Hong-shi Zong[2,†]
[1]School of Physics, Southeast University, Nanjing 211189, China
[2]Department of Physics, Nanjing University, Nanjing 211193, China

(Received 7 April 2019; published 13 September 2019)

The influence of finite-volume effects on dynamical chiral symmetry breaking of thermal QED_3 is investigated. We show that the chiral symmetry gets restored at all temperatures when the size of system is less than some certain value $L_c' = 189$; the critical temperature of chiral phase transition generally increases with the size of the system and the critical temperature when the system volume tends to infinity is slightly less than that in the case of infinite volume.

DOI: 10.1103/PhysRevD.100.054012

I. INTRODUCTION

Quantum electrodynamics in $2+1$ dimensions (QED_3) has been widely studied for many years in the case of Abelian system which exhibits some typical nonperturbative features, such as dynamical chiral symmetry breaking (DCSB) and confinement [1–10]. In addition, because of the superrenormalizable nature and the absence of self-coupled boson, the calculation in QED_3 is relatively simple. Hence, it is treated as a toy model of quantum chromodynamics. Moreover, the model has been applied to the study of some system in condensed matter physics. Especially, QED_3 can be regarded as a model for the high-T_c superconductivity and fractional quantum Hall effect [11–14]. Since the discovery of graphene, QED_3 has been a great success in explaining the planar system [15–19].

The study of DCSB in QED_3 has been an active subject for the past 30 years since Appelquist *et al.* found that the DCSB of QED_3 at zero temperature and density disappears when the number of massless fermion flavors exceeds a critical number $N_c \approx 3.24$ [20]. They reached this conclusion by solving the lowest order of Dyson-Schwinger equation (DSE) for the fermion propagator. Later, extensive analytical and numerical investigations showed that the DCSB in QED_3 still remains after including higher order corrections to the DSE and N_c lies between 3 and 4 [21–23]. To further verify the value of N_c, in recent years some groups have used other methods to obtain N_c values exceeding 2.8 [24–26]. Nevertheless, the conclusions above are obtained at infinite volume and may change at finite size. Due to the finite volume of physical objects in reality, the effect of finite volume on phase transition could be of particular importance. A breakthrough in the study of chiral phase transition (CPT) in QED_3 at finite volume was illustrated in the paper of Ref. [27]. The authors adopted the DSE with rainbow approximation and found that the critical number of fermion flavors in QED_3 at finite volume reduces to the value below 1.5 which is significantly less than that in infinite volume. It should be noted here that Ref. [27] only deals with the effects of the finite volume on the CPT of QED_3 in the case of zero temperature, so a natural problem arises: what will happen to the finite temperature situation?

It is worth mentioning that with the finite temperature involved and mandated by the well-known Coleman-Mermin-Wagner theorem [28], there is no DCSB in thermal QED_3 and hence no rigorous CPT, which is well defined in $(3+1)$-dimensional system at finite temperature. This theorem is usually interpreted as the absence of any crystals in a two-dimensional system. Here, it should be noted that the theorem is only proved to hold in an infinite volume. For the case of a finite size system, it may no longer hold. Actually, a recent research indicates that, in a small two-dimensional system with only a few hundred particles, the crystals do exist [29]. As the system size increases, the disorder of the particle position enlarges and eventually the long-lived crystals are destroyed. This is to say, the continuous symmetry breaking can exist in a two-dimensional system with finite size. Thus, the DCSB may occur in a finite size thermal QED_3 system as well.

Based on the above considerations, we investigate the CPT of thermal QED_3 in finite volume. This paper is organized as follows: in Sec. II, we introduce the DSEs formulation of QED_3 at finite temperature and volume; Sec. III is devoted to the discussion of boson polarization in the finite volume. We then present our numerical results in Sec. IV. Finally, we conclude in Sec. V.

II. ORDER OF CHIRAL PHASE TRANSITION

The Lagrangian for massless QED_3 with a general covariant gauge in Euclidean space can be written as

*fenght@seu.edu.cn
†zonghs@nju.edu.cn

$$\mathcal{L} = \bar{\psi}(\not{\partial} + ie\not{A} - m)\psi + \frac{1}{4}F_{\sigma\nu}^2 + \frac{1}{2\xi}(\partial_\sigma A_\sigma)^2, \quad (1)$$

where the four-component spinor ψ is the massless fermion field, ξ is the gauge parameter. In the absence of the mass term $m\bar{\psi}\psi$, this system has chiral symmetry and the symmetry group is $U(2)$. The original $U(2)$ symmetry reduces to $U(1) \times U(1)$ when the massless fermion acquires a nonzero mass due to nonperturbative effects and order parameter for the CPT no longer equals zero. At zero temperature and density, the parameter in infinite volume is defined trivially via

$$\langle\bar{\psi}\psi\rangle = \mathrm{Tr}[S(x\equiv 0)] = \int \frac{\mathrm{d}^3 p}{(2\pi)^3}\frac{4B(p^2)}{A^2(p^2)p^2 + B^2(p^2)}. \quad (2)$$

The two functions $A(p^2)$ and $B(p^2)$ in the above equation are related to the inverse fermion propagator

$$S^{-1}(p) = i\gamma\cdot pA(p^2) + B(p^2). \quad (3)$$

To obtain the fermion propagator, we employ the non-perturbation DSE method and numerically solve the fermion gap equation

$$S^{-1}(p) = i\gamma\cdot p + \int \frac{\mathrm{d}^3 k}{(2\pi)^3}\gamma_\rho S(k)\gamma_\nu D_{\rho\nu}(p-k), \quad (4)$$

where the natural unit $e^2 = 1$ is used.

Apart from zero temperature and zero density, the O(3) symmetry of the system reduces to O(2). Without regard to chemical potential, the fermion propagator is generally written as

$$S^{-1}(T,P) = i\vec{\gamma}\,\vec{P}\,A_\parallel(P^2) + i\varpi_n\gamma_0 A_0(P^2) + B(P^2), \quad (5)$$

where $\varpi_n = (2n+1)\pi T$.

Now, let us give a short review of some studies on the effect of the wave function renormalization factor $A_\parallel$ and A_0. In the past, the lowest order approximation, i.e., $A_\parallel = A_0 = 1$, is often adopted to calculate the critical fermion flavor, and the results show that although the influence of $A_\parallel, A_0$ can change the numerical results, the low order approximation of DSE of fermion propagator still contains qualitative nonperturbative properties of QED_3 at zero temperature. However, just as the Refs. [30,31] suggested, one should treat renormalization factor $A_\parallel$ and A_0 carefully at finite temperature. Indeed, it is important to obtain $A_\parallel, A_0$ beyond the lowest order approximation in the case of finite temperature. But the numerical calculation is complex, and it is difficult to obtain stable solutions. Therefore, as the first step to study the CPT at finite volume and to obtain qualitative results, the lowest order approximation $A_\parallel = A_0 = 1$ will still be adopted in this work.

At infinite volume, the integral equation for the dynamically generated fermion self-energy function of thermal QED_3 reads

$$\begin{aligned} B(P^2) &= \sum_n \int \frac{\mathrm{d}^2 K}{(2\pi)^2}\frac{2TB(K^2)}{[\varpi_n^2 + \mathcal{E}^2(K^2)][Q^2 + \Pi(Q^2)]} \\ &= \int \frac{\mathrm{d}^2 K}{(2\pi)^2}\frac{B(K^2)\tanh\frac{\mathcal{E}(K^2)}{2T}}{\mathcal{E}(K^2)[Q^2 + \Pi(Q^2)]}, \end{aligned} \quad (6)$$

where $\mathcal{E}(K^2) = \sqrt{K^2 + B^2(K^2)}$ and the Matsubara frequency is summed analytically. The corresponding boson polarization is given as

$$\Pi(Q^2) = \frac{T}{\pi}\int_0^1 \mathrm{d}x \ln\left(4\cosh^2\frac{\sqrt{x(1-x)Q^2}}{2T}\right). \quad (7)$$

Based on the iterative technique of numerical calculation, we find that the value of $B(P^2)$ in Eq. (6) vanishes at $T_c^\infty \approx 2.47 \times 10^{-2}$ [32].

As the volume of the system becomes limited, the photon and fermion fields will be confined in a potential well in spatial directions. To discuss the volume effect, we set the well to be of equal length in the two dimensions, $L_1 = L_2 = L$. Following the discussion in Ref. [27], we adopt the antiperiodic boundary conditions for the fermion fields and write the momentum integral as a sum of Matsubara modes. Then, the lowest order of DSE of the fermion propagator at finite volume is written as

$$B(\omega_{m1}^2,\omega_{m2}^2) = \frac{1}{L^2}\sum_{n_1,n_2=-M}^{M}\frac{B(\omega_{n1}^2,\omega_{n2}^2)\tanh\frac{\mathcal{E}(\omega_{n1}^2,\omega_{n2}^2)}{2T}}{\mathcal{E}(\omega_{n1}^2,\omega_{n2}^2)[Q_v^2 + \Pi(Q_v^2)]}, \quad (8)$$

with $\omega_n = (2n+1)\pi/L$ and $Q_v^2 = (\omega_{m1} - \omega_{n1})^2 + (\omega_{m2} - \omega_{n2})^2$. Once the polarization of the photon is obtained, we can calculate the fermion self-energy equation by the iteration method to analyze the chiral phase transition of thermal QED_3.

III. BOSON POLARIZATION IN FINITE VOLUME

To obtain the boson polarization at finite volume, we first revisit the boson polarization tensor in one-loop order at zero temperature and zero density at infinite volume

$$\begin{aligned} \Pi_{\sigma\nu}(q) &= -\int \frac{\mathrm{d}^3 k}{(2\pi)^3} Tr\left[\frac{\gamma_\sigma(-i\not{k})\gamma_\nu(-i\not{p})}{k^2 p^2}\right] \\ &= 4\int \frac{\mathrm{d}^3 k}{(2\pi)^3}\left[\frac{k_\sigma p_\nu + k_\nu p_\sigma - pk\delta_{\sigma\nu}}{k^2 p^2}\right], \end{aligned}$$

where $q = p - k$. Setting $u = k + qx$, we can write the above equation as

$$\Pi_{\sigma\nu}^{m'} = 4\int \frac{\mathrm{d}^3k}{(2\pi)^3}\int_0^1 \mathrm{d}x \frac{I_{\sigma\nu}}{[u^2+x(1-x)q^2]^2}, \tag{9}$$

where

$$I_{\sigma\nu} = 2x(1-x)(q^2\delta_{\sigma\nu} - q_\sigma q_\nu) - [u^2+x(1-x)q^2]\delta_{\sigma\nu} + 2u_\sigma u_\nu + (1-2x)(u_\sigma q_\nu + u_\nu q_\sigma - uq\delta_{\sigma\nu}). \tag{10}$$

At finite temperature, $u=(u_0,U)$, $u_0 = 2(n+xm'+\frac{1}{2})\pi T$. Following the approximation in the chiral limit [30], we also keep the zero frequency value of the polarization ($q_0=0$) and then arrive at

$$\begin{aligned}\Pi(Q) &= 4T\int\frac{\mathrm{d}^2U}{(2\pi)^2}\int_0^1 \mathrm{d}x \sum_n\left[\frac{1}{u_0^2+U^2+x(1-x)q^2} - \frac{2[U^2+x(1-x)q_0^2]-(1-2x)u_0q_0}{[u_0^2+U^2+x(1-x)q^2]^2}\right]\\ &= 2\int\frac{\mathrm{d}^2U}{(2\pi)^2}\int_0^1 \mathrm{d}x\left\{\frac{\tanh(\frac{y}{2T})}{y} - \frac{U^2}{y^2}\left[\frac{\tanh(\frac{y}{2T})}{y} - \frac{\mathrm{sech}^2(\frac{y}{2T})}{2T}\right]\right\},\end{aligned}$$

with $y=\sqrt{U^2+x(1-x)Q^2}$.

As the system shape becomes a square box with side length of L, the photon polarization of the system transforms into the following form:

$$\Pi(Q_v^2) = \Pi_0(\omega'^2_{m1},\omega'^2_{m2}) = \frac{2}{L^2}\sum_{n1,n2=-M}^{M}\int_0^1 \mathrm{d}x \times\left\{\frac{\tanh(\frac{y'}{2T})}{y'} - \frac{U'^2}{y'^2}\left[\frac{\tanh(\frac{y'}{2T})}{y'} - \frac{\mathrm{sech}^2(\frac{y'}{2T})}{2T}\right]\right\}, \tag{11}$$

with $U'^2 = \omega_{n1}^2+\omega_{n2}^2$, $Q_v^2 = \omega'^2_{m1}+\omega'^2_{m2}$ and $y' = \sqrt{U'^2+x(1-x)Q_v^2}$. Unlike the behavior of fermion, the photon at finite volume reveals the periodic boundary conditions and the Matsubara frequency gives $\omega'_m = 2m\pi/L$. In a finite volume, boson is equivalent to being in a one-dimensional infinite potential well for any dimension and the minimum energy of boson should not be zero, which means that the corresponding Matsubara frequency of the boson should not be zero, i.e., $m \neq 0$. The corresponding photon polarization value will depend on a series of discrete points. As a general discussion, we choose two lengths $L=500$ and 2000, and discuss the photon polarization values calculated with different upper bounds. The typical dependence on the Q_v^2 can be found in Fig. 1. We can see that the photon polarization with finite volume in the small momentum region are almost equal to that in the infinite volume. However, in the large momentum region, the small upper bound yields a numerical result that the photon polarization value deviates significantly from Eq. (7); as the upper bound of the sum increases, the value becomes closer to the case of infinite volume. Further, we choose the upper limit $M=250$ of the summation and calculate the dependence of photon polarization on different sizes and plot the results in Fig. 2. We find that the boson polarization in the small momentum

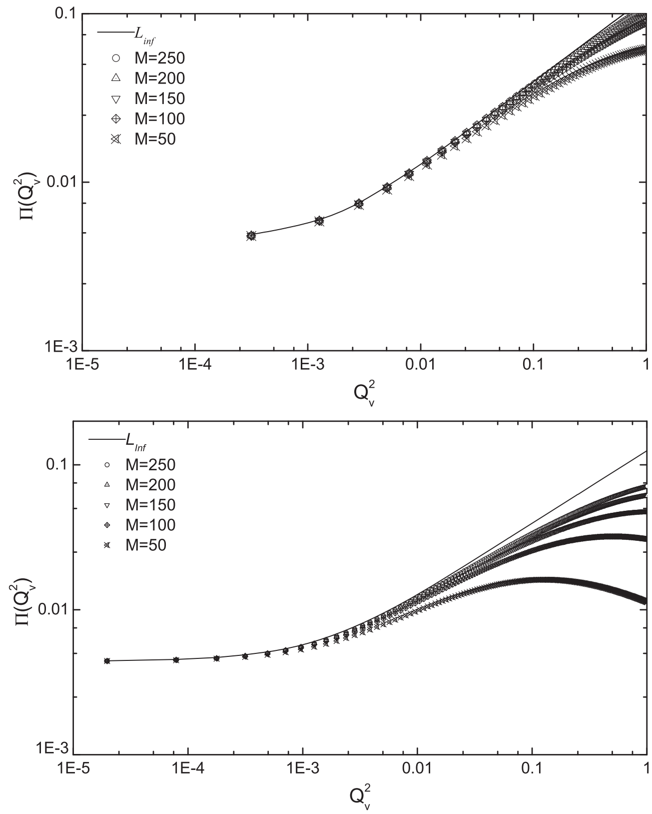

FIG. 1. The dependence of boson polarization value on the summation upper limit at $L=500$ (top) and $L=2000$ (bottom) at $T=0.01$. As a general discussion, we only give the points when $m_1=m_2$ of $\Pi(Q_v^2)$, and the solid line L_{inf} illustrates the behavior of Eq. (7).

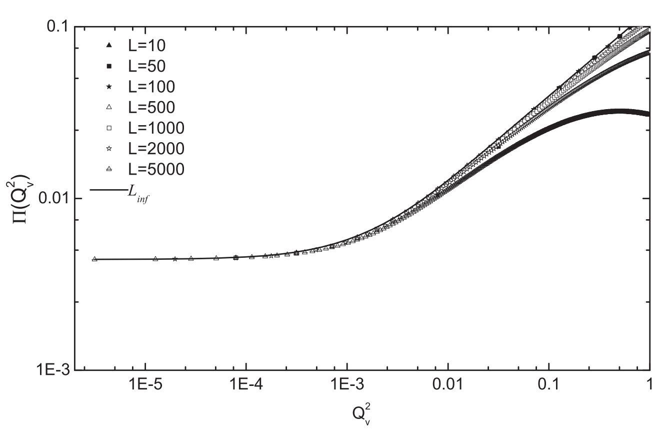

FIG. 2. The boson polarization value with a range of volume at the summation upper limit $M=250$ at $T=0.01$.

region is in good agreement with the numerical results of Eq. (7), while the finiteness of the upper bound results in large deviations at large momentum region. This suggests that for a larger L, we should choose a larger value for M accordingly to preserve the numerical accuracy of Eq. (11). We expect that as the upper bound of the sum increases to infinity, the photon polarization at finite volume can be described by an expression under infinite volume, the difference being that the corresponding momentum is continuous at $L \to \infty$, while the momentum under finite volume is discrete.

IV. NUMERICAL RESULTS

To analyze the CPT of thermal QED_3 at finite size, we next calculate the self-energy with Eq. (8) by iteration method. In the calculation, we need to select an upper limit of the summation. Based on the finding at the end of previous section, we choose a size-related sum of the upper limit $M = M_1 = \frac{L}{2\pi}$. The dependence of fermion self-energy on the selection of the upper bound of the summation can be seen in Fig. 3. We can see that as we increase the upper bound of the summation, the calculated self-energy also increases. However, when the upper limit of the sum exceeds M_1, the self-energy solution starts to converge. Moreover, under the influence of the finite volume effect, the fermion self-energy still decreases with the increase of momentum. Therefore, the value of self-energy $B_{00} \equiv B(\omega_0^2, \omega_0^2)$ can also be treated as the order parameter to determine CPT.

On the basis of selecting M_1 as the upper limit of the sum, we calculate the self-energy of fermion at (1) different L's with same T and (2) different T's with same L. The typical behavior of self-energy with momentum dependence can be seen in Fig. 4. We can find that as the size of the system decreases, the corresponding fermion self-energy value decreases. When the size drops to a critical value L_c, the self-energy decreases to zero. Similarly, the dependence of self-energy on temperature is analyzed at a fixed size in the lower plot of Fig. 4. We find that as the temperature rises, the self-energy diminishes to zero at the critical temperature T_c.

Based on the above discussion, we studied the effect of size on critical temperature. The result can be seen in the Fig. 5. We find that for any size, as the temperature rises, B_{00} diminishes to zero at critical temperature T_c. The value of T_c is obviously dependent on the size L, i.e., the larger the size the higher the T_c. Further, we analyzed the influence of the size change on DCSB at different

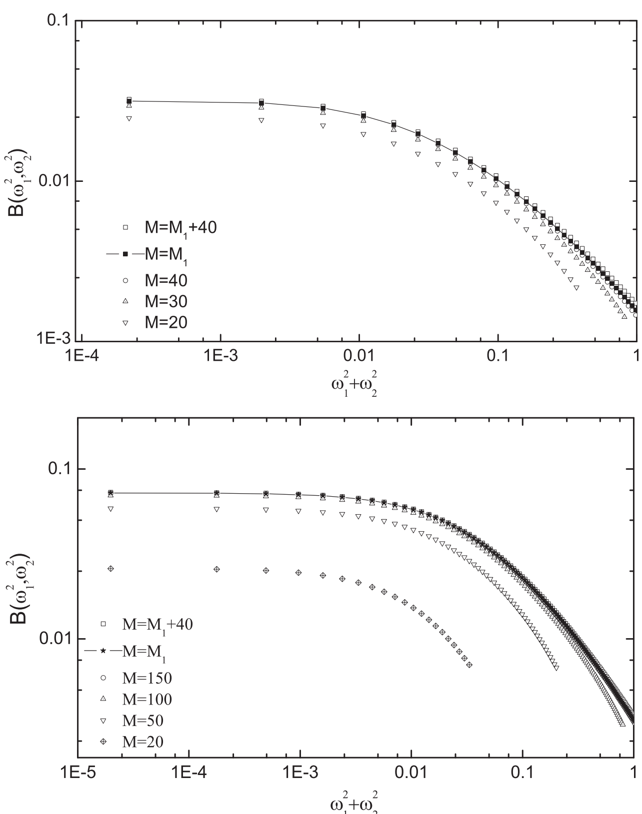

FIG. 3. The dependence of fermion self-energy on the summation upper limit $L = 300$ (top) and $L = 1000$ (bottom) at $T = 0.01$ (where $\omega_1 = \omega_2$ is adopted).

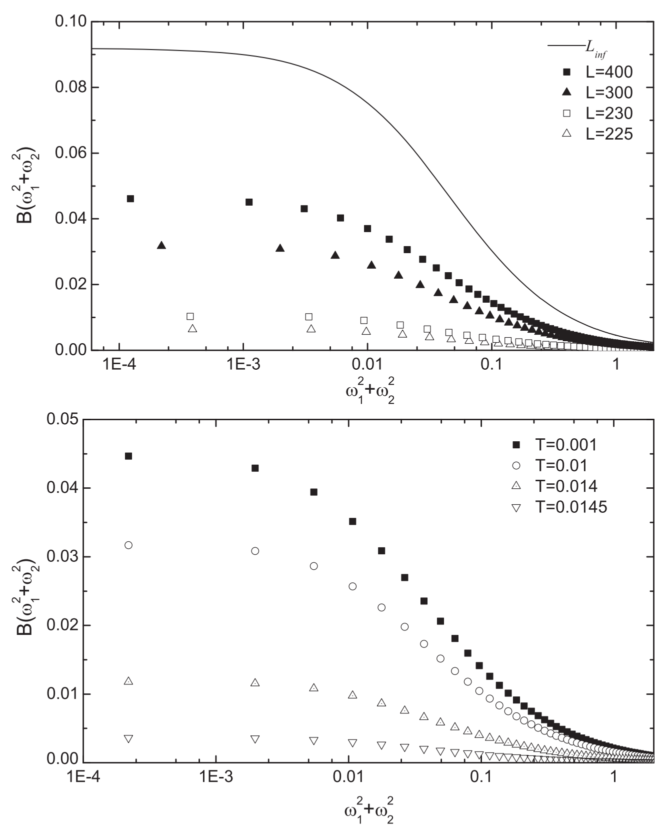

FIG. 4. The typical dependence of fermion self-energy on the volume size at $T = 0.01$ (top) and on temperature at $L = 300$ (bottom), where the solid line L_{inf} gives the behavior of B at infinite volume.

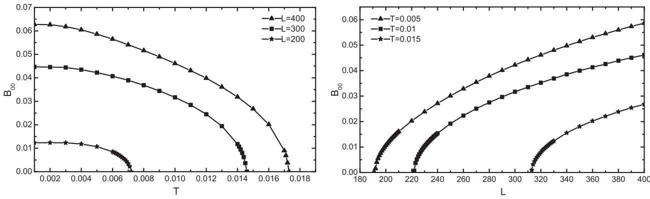

FIG. 5. The relation between order parameter and temperature with several volume size (left) and with different temperature (right).

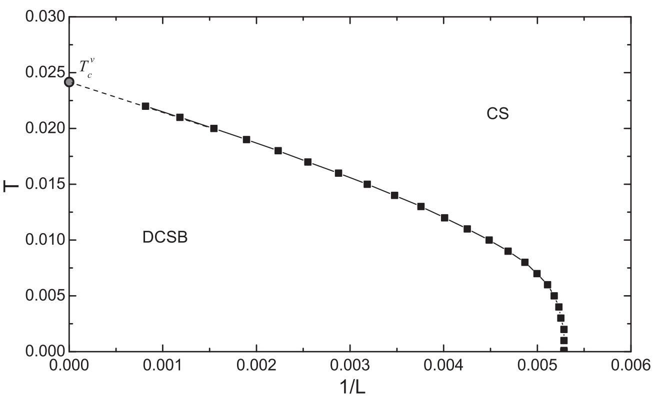

FIG. 6. The relation of inverse volume size $1/L$ and the corresponding critical temperature T.

temperatures. From Fig. 5, we see that for any temperature, B_{00} gradually decrease as the size decreases, and it reduces to zero at a critical value L_c.

Finally, we give the critical temperature of chiral phase transition of the thermal QED_3 at finite size in Fig. 6. From the figure, we can see that when L is less than a critical value $L_c' \simeq 189$, the chiral symmetry of thermal QED_3 restores for any temperature. As the size exceeds 189, the critical temperature of the system starts to rise. Near $L_c' = 189$, the critical temperature increases rapidly with the size of the system. As the size increases further, the increase in critical temperature become slower. An interesting phenomenon is that in a relatively large size, there is an approximate linear relationship between the reciprocal of the system size and the critical temperature. When $1/L \to 0$, i.e., the size tends to infinity, we find that the critical temperature tends to $T_c^v \approx 2.42 \times 10^{-2}$ which is slightly less than T_c^∞.

V. CONCLUSIONS

In this paper, we adopt the Dyson-Schwinger equation to study the influence of finite size effect on chiral phase transition in thermal QED_3. Our results show that the critical temperature of chiral phase transition decreases significantly with the decrease of the system size. Especially, when the system size is less than a critical value, the chiral symmetry of the system will no longer be broken. This finding verifies Weinberg's view that symmetry breaking can only occur in systems with a certain large size [33]. On the other hand, as the size increases, the critical temperature rises, but the magnitude of the increase gradually decreases, and tends to the critical temperature value in the infinity volume.

ACKNOWLEDGMENTS

We would like to thank Prof. Guo-Zhu Liu for his helpful discussions. This work is supported in part by the National Natural Science Foundation of China (under Grants No. 11475085, No. 11535005, and No. 11690030) and Nation Major State Basic Research and Development of China (Grant No. 2016YFE0129300).

[1] D. Nash, Phys. Rev. Lett. **62**, 3024 (1989).
[2] J. S. Ball and T. W. Chiu, Phys. Rev. D **22**, 2542 (1980).
[3] D. C. Curtis and M. R. Pennington, Phys. Rev. D **42**, 4165 (1990).
[4] T. Appelquist, J. Terning, and L. C. R. Wijewardhana, Phys. Rev. Lett. **75**, 2081 (1995).
[5] H. T. Feng, B. Wang, W. M. Sun, and H. S. Zong, Phys. Rev. D **86**, 105042 (2012).
[6] H. T. Feng, B. Wang, W. M. Sun, and H. S. Zong, Eur. Phys. J. C **73**, 2444 (2013).
[7] H. T. Feng, J. F. Li, Y. M. Shi, and H. S. Zong, Phys. Rev. D **90**, 065005 (2014).
[8] N. Zerf, P. Marquard, R. Boyack, and J. Maciejko, Phys. Rev. B **98**, 165125 (2018).
[9] B. Ihrig, L. Janssen, L. N. Mihaila, and M. M. Scherer, Phys. Rev. B **98**, 115163 (2018).
[10] S. Hands, Phys. Rev. D **99**, 034504 (2019).
[11] W. Rantner and X. G. Wen, Phys. Rev. Lett. **86**, 3871 (2001).
[12] M. Franz and Z. Tesanovic, Phys. Rev. Lett. **87**, 257003 (2001); I. F. Herbut, Phys. Rev. Lett. **88**, 047006 (2002); Phys. Rev. B **66**, 094504 (2002); Phys. Rev. Lett. **94**, 237001 (2005).
[13] X. G. Wen and A. Zee, Phys. Rev. Lett. **69**, 1811 (1992).
[14] G. Z. Liu and G. Cheng, Phys. Rev. B **66**, 100505(R) (2002).
[15] J. Wang, P. L. Zhao, J. R. Wang, and G. Z. Liu, Phys. Rev. B **95**, 054507 (2017).
[16] J. R. Wang and G. Z. Liu, Phys. Rev. B **89**, 195404 (2014).
[17] J. R. Wang, G. Z. Liu, and C. J. Zhang, Phys. Rev. D **91**, 045006 (2015).

[18] A. V. Kotikov and S. Teber, Phys. Rev. D **94**, 114010 (2016).
[19] S. Teber and A. V. Kotikov, Theor. Math. Phys. **190**, 446 (2017).
[20] T. Appelquist, D. Nash, and L. C. R. Wijewardhana, Phys. Rev. Lett. **60**, 2575 (1988).
[21] P. Maris, Phys. Rev. D **54**, 4049 (1996).
[22] A. Bashir, C. Calcaneo-Roldan, L. X. Gutierrez-Guerrero, and M. E. Tejeda-Yeomans, Phys. Rev. D **83**, 033003 (2011).
[23] C. S. Fischer, R. Alkofer, T. Dahm, and P. Maris, Phys. Rev. D **70**, 073007 (2004).
[24] V. P. Gusynin and P. K. Pyatkovskiy, Phys. Rev. D **94**, 125009 (2016).
[25] A. V. Kotikov and S. Teber, Phys. Rev. D **94**, 114011 (2016).
[26] A. V. Kotikov, V. I. Shilin, and S. Teber, Phys. Rev. D **94**, 056009 (2016).
[27] T. Goecke, C. S. Fischer, and R. Williams, Phys. Rev. B **79**, 064513 (2009).
[28] N. D. Mermin and H.Wagner, Phys. Rev. Lett. **17**, 1133 (1966).
[29] B. Illing, S. Fritschi, H. Kaiser, C. L. Klix, G. Maret, and Peter Keim, Proc. Natl. Acad. Sci. U.S.A. **114**, 1856 (2017).
[30] N. Dorey and N. E. Mavromatos, Nucl. Phys. **B386**, 614 (1992).
[31] I. J. R. Atichison, N. Dorey, M. Klein-Kreisler, and N. E. Mavromatos, Phys. Lett. B **294**, 91 (1992).
[32] H. T. Feng, Mod. Phys. Lett. A **27**, 1250209 (2012).
[33] S. Weinberg, *The Quantum Theory of Fields*, Volume II Modern Application (Cambridge University Press, Cambridge, United Kingdom, 1996).